

LA-UR- 09-0418

Approved for public release;
distribution is unlimited.

Title:

Dislocation density evolution during high pressure torsion of a nanocrystalline Ni-Fe alloy

Author(s):

Y. B. Wang, J. C. Ho, Y. Cao, X. Z. Liao, H. Q. Li, Y. H. Zhao, E.J. Lavernia, S. P. Ringer, and Y. T. Zhu

Intended for:

publication

Applied Physics Letters



Los Alamos National Laboratory, an affirmative action/equal opportunity employer, is operated by the Los Alamos National Security, LLC for the National Nuclear Security Administration of the U.S. Department of Energy under contract DE-AC52-06NA25396. By acceptance of this article, the publisher recognizes that the U.S. Government retains a nonexclusive, royalty-free license to publish or reproduce the published form of this contribution, or to allow others to do so, for U.S. Government purposes. Los Alamos National Laboratory requests that the publisher identify this article as work performed under the auspices of the U.S. Department of Energy. Los Alamos National Laboratory strongly supports academic freedom and a researcher's right to publish; as an institution, however, the Laboratory does not endorse the viewpoint of a publication or guarantee its technical correctness.

Dislocation Density Evolution during High Pressure Torsion of a Nanocrystalline Ni-Fe Alloy

Y. B. Wang,¹ J. C. Ho,¹ Y. Cao,¹ X. Z. Liao,^{1,a)} H. Q. Li,² Y. H. Zhao,³ E.J. Lavernia,³ S.
P. Ringer,⁴ and Y. T. Zhu⁵

¹School of Aerospace, Mechanical & Mechatronic Engineering, The University of
Sydney, NSW 2006, Australia

²Los Alamos National Laboratory, Los Alamos, New Mexico 87545, USA

³Department of Chemical Engineering and Materials Science, University of California at
Davis, Davis, CA 95616, USA

⁴Australian Key Centre for Microscopy & Microanalysis, The University of Sydney,
NSW 2006, Australia

⁵Department of Materials Science & Engineering, North Carolina State University,
Raleigh, NC 27695-7919, USA

^{a)} Corresponding author. Email: xliao@usyd.edu.au

Abstract:

High-pressure torsion (HPT) induced dislocation density evolution in a nanocrystalline Ni-20wt.%Fe alloy was investigated using X-ray diffraction and transmission electron microscopy. Results suggest that the dislocation density evolution is different from that in coarse-grained materials. An HPT process first reduces the dislocation density within nanocrystalline grains and produces a large number of dislocations located at small-angle subgrain boundaries that are formed via grain rotation and coalescence. Continuing the deformation process eliminates the subgrain boundaries but significantly increases the dislocation density in grains. This phenomenon provides an explanation of the mechanical behavior of some nanostructured materials.

The density, distribution, interaction, annihilation and accumulation of dislocations play a key role in determining the mechanical properties of materials. Manipulating dislocation density and distribution via appropriate processing including annealing and cold work can therefore change the mechanical properties of materials. It has been well known that conventional coarse-grained metals and alloys can be softened by annealing and strengthened by cold work.¹ Annealing reduces the dislocation density in the materials while cold work increases the dislocation density and therefore results in work hardening. On the other hand, increase in dislocation density by cold work reduces the capability of further dislocation accumulation, and this decreases the ductility of the materials. In contrast, the processing-property relationship of some nanostructured materials has been reported completely different from that of conventional coarse-grained materials. For example, nanostructured Al can be strengthened by annealing and softened by deformation.² The unique processing-property relationship of nanostructured materials is believed closely related to the unique dislocation behavior/deformation mechanisms in the nanostructured materials.

The deformation mechanisms of nanostructured materials are significantly different from that of coarse-grained materials. For example, for materials with grain sizes of tens of nanometers, partial dislocation emissions from grain boundaries play a significant role in plastic deformation.^{3,4,5,6} The difference in deformation mechanisms is expected to affect the dislocation density evolution during plastic deformation and subsequently to affect the mechanical behaviors of the materials. *In-situ* x-ray diffraction peak profile analysis of nanocrystalline Ni, which has an average grain size of 26 nm, under uniaxial tensile straining⁷ has revealed that grain boundaries act as the source and sink for

dislocations, leaving no additional dislocation debris, as predicted by molecular dynamics simulations,⁸ in nanocrystalline grains. This leads to the absence of substantial work hardening in nanocrystalline metals.⁷

Recent experimental results have evidenced grain growth of nanocrystalline metals and alloys during plastic deformation.^{9,10,11,12} The grain growth occurs via grain rotation and coalescence for nanocrystalline grains of the sizes of ~ 20 nm.^{13,14,15} The grain rotation process results in the formation of large amount of small-angle subgrain boundaries with high density of dislocations located at the boundaries.¹⁵ It has not been clear how these boundary dislocations will change the global dislocation behavior in the materials and subsequently affect the deformation behavior of the materials. To uncover the effect of the deformation induced grain rotation and coalescence on the global dislocation behavior in nanostructured materials, we have applied x-ray diffraction peak profile analysis and high-resolution transmission electron microscopy (TEM) to investigate the evolution of dislocation density and distribution of nanocrystalline Ni-20wt.%Fe disks processed by the high-pressure torsion (HPT) technique.

The as-received NiFe alloy used in this investigation was produced via electrochemical deposition.¹⁶ Disks with a thickness around 0.7 mm and a diameter of 10 mm were processed using HPT for 1 and 9 revolutions, respectively, under 3.8 GP at room temperature and a very low strain rate of about 10^{-2} s⁻¹. X-ray diffraction (XRD) experiments were carried out using a Siemens D5000 diffractometer. Details of the XRD peak profile analysis method have been described in ref.17. A coarse-grained NiFe sample obtained by annealing the as-received alloy at 600°C for two hours followed by quenching in water was used as the XRD peak broadening reference. TEM observations

were carried out in a Philips CM12 microscope working at 120 keV and a JEOL 3000F microscope operating at 300 keV.

Figure 1 shows XRD patterns of the annealed, the as-received, the 1-revolution HPT, and the 9-revolution HPT samples. All samples are of the same face-centered-cubic structure. XRD peak profile analysis suggests that the dislocation densities in the as-received sample, the 1-revolution HPT sample, and the 9-revolution HPT sample are $8.3 \times 10^{14} \text{ m}^{-2}$, $5.7 \times 10^{14} \text{ m}^{-2}$, and $10.2 \times 10^{14} \text{ m}^{-2}$, respectively, indicating that the dislocation density *within* the grains of the NiFe alloy does not evolve monotonously but decreases first and then increases. This dislocation density evolution process is completely different from that in coarse-grained materials.¹⁸ Plastic deformation induced dislocation density reduction in a nanocrystalline material has recently been reported by Li et al.¹⁹ during a cold rolling process. However, the latter stage of dislocation density evolution, i.e., deformation induced dislocation density increase, has never been reported before. Note that the value of dislocation density calculated from XRD peak profile analysis is usually only qualitative. However, the trend of dislocation density evolution is valid if it is measured and analyzed in a consistent way.

The average grain size of the as-received sample is about 22 nm. The dislocation density in the as-received sample obtained from statistical analysis of high-resolution TEM images is $1.2 \times 10^{16} \text{ m}^{-2}$, i.e., close to 5 dislocations in each grain in average. An example of a grain in the as-received sample with a few dislocations in the grain is shown in Fig. 2. Such a high density of dislocations in nanocrystalline grains is very unstable and the dislocations tend to glide to and disappear at grain boundaries when external force is available to activate dislocation motion.²⁰ This is the reason that results in

reduction of the dislocation density at the initial stage of HPT of the nanocrystalline Ni-Fe alloy. Statistical analysis of high-resolution TEM images suggests that the dislocation density *within* the grains of the 1-revolution TEM sample is $6.4 \times 10^{15} \text{ m}^{-2}$, which is about half of the original density.

In addition to reducing the dislocation density within grains, the HPT process also results in grain growth via grain rotation, forming a large amount of small-angle subgrain boundaries within the newly formed large grains and high densities of dislocations located at the subgrain boundaries. Figures 3(a) and 3(b) show a bright-field diffraction contrast TEM image and a high-resolution TEM image of the 1-revolution HPT sample, respectively. The grain sizes of the sample are in the range of $40 \sim 250 \text{ nm}$ with an average grain size of $\sim 95 \text{ nm}$. Atoms at the subgrain boundaries are re-arranged and high densities of dislocations formed at the subgrain boundaries to accommodate the geometrical misorientation between neighboring subgrains. The grain boundary dislocations are clearly seen in the bright-field TEM image as dotted points in Fig. 3(a) and in the high-resolution TEM image in Fig. 3(b). Note that these boundary dislocations cannot be fully accounted by x-ray diffraction because dislocations located at subgrain boundaries do not produce as much elastic strain as those in the grain interior. Including the boundary dislocations increases the dislocation density in the 1-revolution HPT sample to about $5.3 \times 10^{16} \text{ m}^{-2}$, almost one order of magnitude higher than the density value that does not include the subgrain boundary dislocations.

With the development of the HPT process, the misorientation angles between neighbouring subgrains decrease gradually to zero and the dislocations that accommodate the misorientation necessarily glide away.²¹ Because the subgrain boundaries exist three-

dimensionally,¹⁵ it is expected that, when boundary dislocations glide through the grains, the dislocations lying on different groups of {111} planes will interact and tangle with each other. This not only hinders the motion of dislocation but also provides sources (e.g., the Frank-Reed sources²²) for dislocation multiplication within grains. As a result, dislocation density in grains is expected to increase significantly. Figure 4 shows a bright-field diffraction contrast TEM image (a) and a high-resolution TEM image (b) of the 9-revolution HPT sample. Small-angle subgrain boundaries no longer exist while random distribution of high density of dislocations is seen clearly. The dislocation density in the grains of the 9-revolution HPT sample is about $4 \times 10^{16} \text{ m}^{-2}$, which is more than 6 times higher than the dislocation density *within* the grains of the 1-revolution sample but is compatible to the density in the 1-revolution HPT sample if dislocations at subgrain boundaries are included.

Note that all the dislocation seen in Fig. 4 are full dislocations (partial dislocations are always associated with stacking faults), suggesting that the mechanism of partial emissions from grain boundaries does not operate during the deformation process. The high density of full dislocations seen in Fig. 4 could be generated from both the interior and the boundaries of grains.

It has been reported that the deformation behaviour of a nanocrystalline Ni-Fe alloy is a function of applied strain:²³ at low strains, deformation is mainly accommodated at grain boundaries, while at high strains, dislocation motion dominates. This phenomenon is consistent with our experimental observations. At the initial stage of a deformation, two phenomena have been observed: (1) dislocation density within nanocrystalline grains decreases, suggesting that there is no dislocation multiplication and that dislocations do

not play any significant role in the deformation, and (2) grain growth occurs through grain rotation and atomic rearrangement at small-angle subgrain boundaries, indicating that the grain boundaries played a significant role at this stage of deformation. Further deformation reduces the misorientation angles between neighbouring subgrains and forces the subgrain boundary dislocations to glide away along different groups of {111} planes, resulting in dislocation tangling that provides additional sources for dislocation multiplication. The dislocation interaction at the later stage of deformation increases significantly not only the dislocation density but also the dislocation storage capability and therefore increases significantly the strength while at the same time retains the ductility of the materials.²³

In summary, our structural investigation of a nanocrystalline Ni-Fe alloy at different stages of the HPT process reveals that the deformation induced dislocation density evolution in the material is different from that seen in coarse grain materials. Briefly, the dislocation density *within* grains first decreased and then increased with increasing HPT strain. These results provide a reasonable explanation of the mechanical behaviour of some nanostructured materials.

The authors are grateful for scientific and technical input and support from the Australian Microscopy & Microanalysis Research Facility node at the University of Sydney. This project is financially supported by the Australian Research Council [Grant No. DP0772880 (Y.B.W., J.C.H, Y. Cao, and X.Z.L.)], the LDRD program of Los Alamos National Laboratory (H.Q.L.), Office of Naval Research [Grant numbers N00014-04-1-0370 and N00014-08-1-0405 (Y.H.Z. and E.J.L.)], and the U.S. DOE IPP program (Y.T.Z.).

References

¹ W. D. Callister, Jr., *Materials Science and Engineering An Introduction*, (John Wiley & Sons, Inc., 2007), pp. 191-199

² X. X. Huang, N. Hansen, and N. Tsuji, *Science* **312**, 249 (2006).

³ X. Z. Liao, F. Zhou, E. J. Lavernia, S. G. Srinivasan, M. I. Baskes, D. W. He, and Y. T. Zhu, *Appl. Phys. Lett.* **83**, 632 (2003)

⁴ X. Z. Liao, Y. H. Zhao, S. G. Srinivasan, Y. T. Zhu, R. Z. Valiev, and D. V. Gunderov, *Appl. Phys. Lett.* **84**, 592 (2004)

⁵ V. Yamakov, D. Wolf, S. R. Phillpot, and H. Gleiter, *Acta Mater.* **50**, 5005 (2002)

⁶ H. Van Swygenhoven, *Science* **296**, 66 (2002)

⁷ Z. Budrovic, H. Van Swygenhoven, P. M. Derlet, S. Van Petegem, and B. Schmitt, *Science* **304**, 273 (2004)

⁸ V. Yamakov, D. Wolf, S. E. Phillpot, A. K. Mukherjee, and H. Gleiter, *Nature Mater.* **1**, 45 (2002)

⁹ K. Zhang, J. R. Weertman, and J. A. Eastman, *Appl. Phys. Lett.* **87**, 061921 (2005)

¹⁰ X. Z. Liao, A. R. Kilmanetov, R. Z. Valiev, H. S. Gao, X. D. Li, A. K. Mukherjee, J. F. Bingert, and Y. T. Zhu, *Appl. Phys. Lett.* **88**, 021909 (2006)

¹¹ G. J. Fan, L. F. Fu, H. Choo, P. K. Liaw, and N. D. Browning, *Acta Mater.* **54**, 4781 (2006)

¹² G. J. Fan, Y. D. Wang, L. F. Fu, H. Choo, P. K. Liaw, Y. Ren, and N. D. Browning, *Appl. Phys. Lett.* **88**, 171914 (2006)

¹³ Z. W. Shan, E. A. Stach, J. M. K. Wiezorek, J. A. Knap, D. M. Follstaedt, and S. X. Mao, *Science* **305**, 654 (2004)

¹⁴ Y. B. Wang, B. Q. Li, M. L. Sui, and S.X. Mao, *Appl. Phys. Lett.* **92**, 011903 (2008)

¹⁵ Y. B. Wang, J. C. Ho, X. Z. Liao, H. Q. Li, S. P. Ringer, and Y. T. Zhu, *Appl. Phys. Lett.* **94**, 011908 (2009)

¹⁶ H. Q. Li and F. Ebrahimi, *Mater. Sci. Eng. A* **347**, 93 (2003).

¹⁷ Y. H. Zhao, Z. Horita, T. G. Langdon, and Y. T. Zhu, *Mater. Sci. Eng. A* **474**, 342 (2008)

¹⁸ F. Dalla Torre, R. Lapovok, J. Sandlin, P.F. Thomson, C.H.J. Davies, and E.V. Pereloma, *Acta Mater.* **52**, 4819 (2004)

¹⁹ L. Li, T. Ungár, Y. D. Wang, G. J. Fan, Y. L. Yang, N. Jia, Y. Ren, G. Tichy, J. Lendvai, H. Choo, and P. K. Liaw, *Scripta Mater.* **60**, 317 (2009)

²⁰ Z. W. Shan, R. K. Mishra, S. A. S. Asif, O. L. Warren, and A. M. Minor, *Nature Mater.* **7**, 115 (2008)

²¹ S. V. Bobylev, M. Yu. Gutkin, and I. A. Ovid'ko, *Acta Mater.* **52**, 3793 (2004)

²² F. C. Frank and W. T. Read, *Phys. Rev.* **79**, 722 (1950)

²³ H. Q. Li, H. Choo, Y. Ren, T. A. Saleh, U. Lienert, P. K. Liaw, and F. Ebrahimi, *Phys. Rev. Lett.* **101**, 015502 (2008)

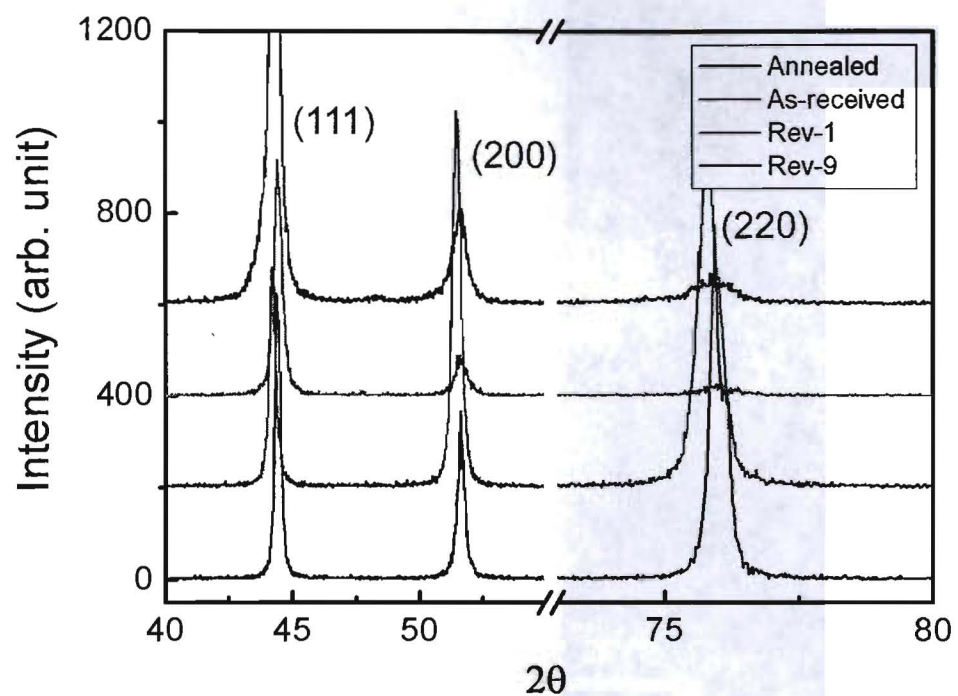


Figure 1. (color). XRD patterns of the annealed (coarse-grained), the as-received (nanocrystalline), the 1-revolution HPT, and the 9-revolution HPT samples.

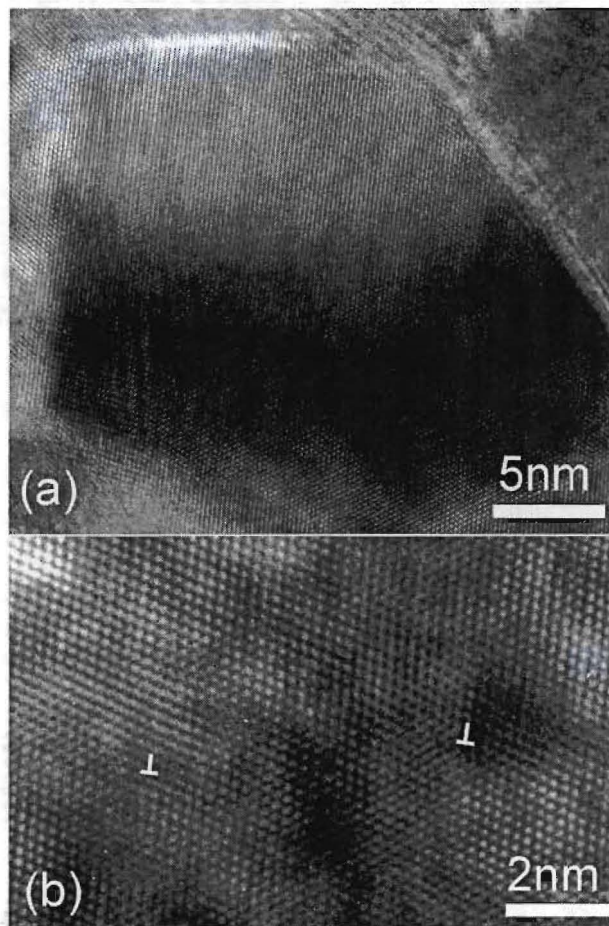


Figure 2. (a) A high-resolution TEM image of a grain in the as-received sample. Dislocation cores are indicated using arrows; (b) a magnified image of part of (a) showing clearly lattice structure. Dislocations are marked with white "T".

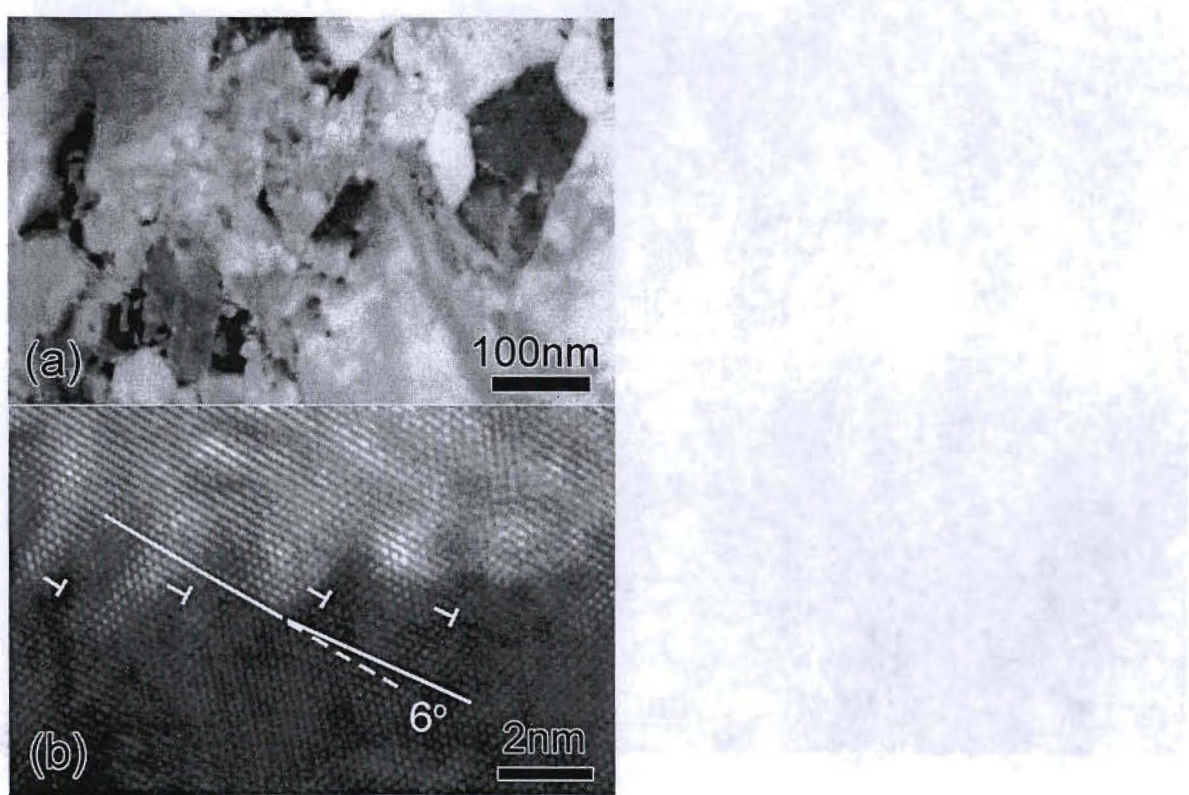


Figure 3. (a) A bright-field TEM image of the 1-revolution HPT sample; (b) A high-resolution TEM image showing high density of dislocations, marked with white "T", located at a small-angle subgrain boundary.

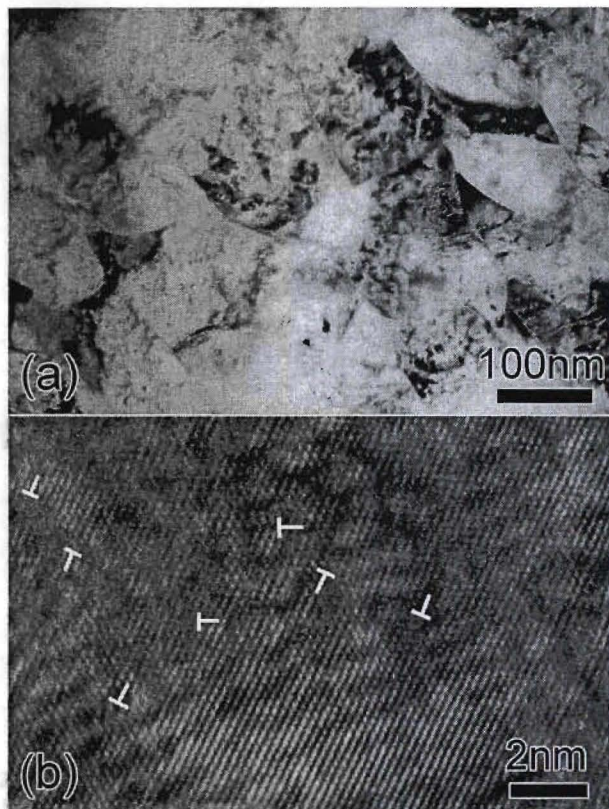


Figure 4. (a) A bright-field TEM image of the 9-revolution HPT sample; (b) A high-resolution TEM image showing random distribution of high density of dislocations which are marked with white “T”.